Photochemical and Electronic Properties of Conjugated Bis(azo) Compounds: An Experimental and Computational Study

Federico Cisnetti,[a] Roberto Ballardini,[b] Alberto Credi,*[a] Maria Teresa Gandolfi,[a] Stefano Masiero,[c] Fabrizia Negri,*[a] Silvia Pieraccini,[c] and Gian Piero Spada[c]

Dedicated to Professor Vincenzo Balzani on the occasion of his birthday

Abstract: We have investigated the photophysical, photochemical and electrochemical properties of two bis(azo) derivatives, (*E*,*E*)-*m*-**1** and (*E*,*E*)-*p*-**1**. The two compounds, which can be viewed as being composed of a pair of azobenzene units sharing one of their phenyl rings, differ only for the relative position of the two azo groups on the central phenyl ring—*meta* and *para* for *m*-**1** and *p*-**1**, respectively. The UV-visible absorption spectra and photoisomerisation properties are noticeably different for the two structural isomers; (*E*,*E*)-*m*-**1** behaves similarly to (*E*)-azobenzene, while (*E*,*E*)-*p*-**1** exhibits a substantial red shift in the absorption bands and a decreased photoreactivity. The three geometric isomers of *m*-**1**, namely the *E*,*E*, *E*,*Z* and *Z*,*Z* isomers, cannot be resolved in a mixture by absorption spectroscopy, while the presence of three distinct species can be revealed by analysis of the absorption changes observed upon photoisomerisation of (*E*,*E*)-*p*-**1**. Quantum chemical ZINDO/1 calculations of vertical excitation energies nicely reproduce the observed absorption changes and support the idea that, while the absorption spectra of the geometrical isomers of *m*-**1** are approximately given by the sum of the spectra of the constituting azobenzene units in their relevant isomeric form, this is not the case for *p*-**1**. From a detailed study on the $E \rightarrow Z$ photoisomerisation reaction it was observed that the photoreactivity of an azo unit in *m*-**1** is influenced by the isomeric state of the other one. Such observations indicate a different degree of electronic coupling and communication between the two azo units in *m*-**1** and *p*-**1**, as confirmed by electrochemical experiments and quantum chemical calculations. The decreased photoisomerisation efficiency of (*E*,*E*)-*p*-**1** compared to (*E*,*E*)-*m*-**1** is rationalised by modelling the geometry relaxation of the lowest π–π* state. These results are expected to be important for the design of novel oligomers and polymers, based on the azobenzene unit, with predetermined photoreactivity.

Keywords: ab initio calculations · absorption spectroscopy · azobenzenes · electrochemistry · photochemistry

Introduction

The physicochemical and structural changes associated with the *E*–*Z* photoisomerisation of azobenzene derivatives[1–4] have been widely exploited to modify chemical systems by means of light stimulation. For instance, such a reaction has been used to modulate the properties of polymers,[5,6] liquid crystals,[7] biomolecules,[8] and dendritic[9] and supramolecular[10,11] systems, as well as to construct molecular-level memories,[12] devices and machines.[13,14]

Molecular systems containing two or more azobenzene units are of interest for at least two reasons: 1) because of their multiphotochromic nature, such compounds can exist in a wealth of different states (up to 2^n, where n is the number of photochromic units), a behaviour that may be useful for molecular-level information processing and storage; 2) the cooperation of the different photoisomerisable units can produce an overall amplification of the geometrical changes related to the *E*–*Z* transformation, leading to new light-induced functions.

Several compounds containing two azobenzene groups have been studied[10,15] in the past, whereby, in most cases,

[a] F. Cisnetti, Dr. A. Credi, Prof. M. T. Gandolfi, Prof. F. Negri
Dipartimento di Chimica "G. Ciamician"
Università di Bologna, via Selmi 2
40126 Bologna (Italy)
Fax: (+39) 051-2099456
E-mail: alberto.credi@unibo.it
fabrizia.negri@unibo.it

[b] Dr. R. Ballardini
Istituto ISOF-CNR, via Gobetti 101
40129 Bologna (Italy)

[c] Dr. S. Masiero, Dr. S. Pieraccini, Prof. G. P. Spada
Dipartimento di Chimica Organica "A. Mangini"
Università di Bologna, via San Donato 15
40127 Bologna (Italy)

 DOI: 10.1002/chem.200305590

the two azobenzenes were found to be basically noninteracting, giving rise to a behaviour determined by the simple superimposition of the properties of the two isolated units. Here we report on the photochemical properties in solution of two compounds, *m*-**1** and *p*-**1**, composed of two *conjugated* azobenzene units.[16] These compounds can be viewed as two azobenzene units sharing one of their phenyl rings, and differ only for the relative position of the two azo groups on the central phenyl ring. Interestingly, *p*-**1** may be considered as the azo analogue of bis(*p*-phenylene vinylene), which is the first member of the oligo(*p*-phenylene vinylene) (OPV) family. Enantiopure derivatives with camphanic ester side groups have been prepared with the aim of obtaining molecular chiral switches for doping nematic liquid crystals. Upon *E*–*Z* photoisomerisation it could be expected the induction of skewed chiral conformations that should modify the pitch of the induced cholesteric phases.[17] Ester substituents in the *para*-position have little or no effect[18] on the photochemical properties of the azobenzene group, and plain azobenzene has been taken as a reference compound for the $E \rightarrow Z$ photoisomerisation.

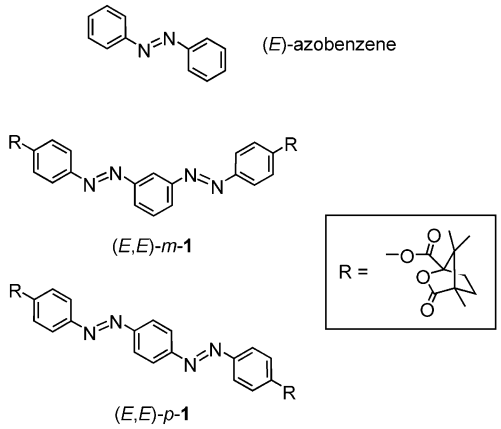

Abstract in Italian: *Sono state studiate le proprietà fotofisiche, fotochimiche ed elettrochimiche di due composti bis(azo), (*E,E*)-*m-***1** *and (*E,E*)-*p-***1***. Tali composti, che possono essere considerati come due unità azobenzene che condividono uno dei loro anelli benzenici, differiscono solo per la posizione relativa dei due gruppi azo sull'anello benzenico centrale (ripettivamente meta e para per* m-***1*** *e* p-***1***). Gli spettri di assorbimento UV-visibile e le caratteristiche di fotoisomerizzazione dei due isomeri strutturali sono notevolmente diverse: (*E,E*)-*m-***1** *si comporta in maniera analoga all'(*E*)-azobenzene, mentre (*E,E*)-*p-***1** *mostra un considerevole spostamento verso il rosso delle bande di assorbimento ed una diminuzione della fotoreattività. I tre isomeri geometrici di* m-***1***, E,E, E,Z *e* Z,Z, *non sono distinguibili in miscela mediante spettroscopia di assorbimento; le variazioni negli spettri di assorbimento osservate durante la fotoisomerizzazione di (*E,E*)-*p-***1***, invece, rivelano la presenza di tre specie distinte. I valori dell'energia di eccitazione verticale ottenuti mediante calcoli quantomeccanici ZINDO/I sono in ottimo accordo con gli spettri di assorbimento. Tali calcoli suggeriscono inoltre che gli spettri di assorbimento degli isomeri geometrici di* m-***1*** *sono sostanzialmente dati dalla somma degli spettri delle unità azobenzene che li costituiscono, ciascuna nella corrispondente forma isomerica, mentre la situazione di* p-***1*** *è completamente diversa. Studi dettagliati sulla reazione di fotoisomerizzazione* E→Z *indicano che la fotoreattività di un'unità azo in* m-***1*** *dipende dalla forma isomerica dell'altra unità. Tali osservazioni mostrano che l'accoppiamento e la comunicazione elettronica tra le due unità azo in* m-***1*** *e* p-***1*** *sono diversi, come confermato da esperimenti elettrochimici e da calcoli quantomeccanici. La diminuzione dell'efficienza di fotoisomerizzazione di (*E,E*)-*p-***1** *rispetto a (*E,E*)-*m-***1** *è interpretata modellando il rilassamento geometrico dello stato* π–π* *più basso. Questi risultati sono rilevanti per la progettazione di nuovi oligomeri e polimeri contenenti unità azobenzene aventi una fotoreattività predeterminata.*

Results and Discussion

Absorption spectra: The absorption spectra of the *E*,*E* isomers of *m*-**1** and *p*-**1** in acetonitrile are shown in Figure 1, together with twice the spectrum of (*E*)-azobenzene. The spectroscopic data are gathered in Table 1. Similarly to that of azobenzene, the spectra of (*E*,*E*)-*m*-**1** and (*E*,*E*)-*p*-**1** exhibit a two-band pattern, with well-separated π–π* and *n*–π* absorption features in the 270–520 nm range, and an intensity which is roughly that expected for the presence of two azobenzene chromophores.[19] The absorption maxima of (*E*,*E*)-*m*-**1** are only slightly shifted relative to azobenzene, and very similar to those of an azobenzene derivative bearing alkyl ester groups in the 4,4′ positions.[18] In contrast, the absorption bands of (*E*,*E*)-*p*-**1** (in particular the π–π* one) are noticeably displaced to lower energy.

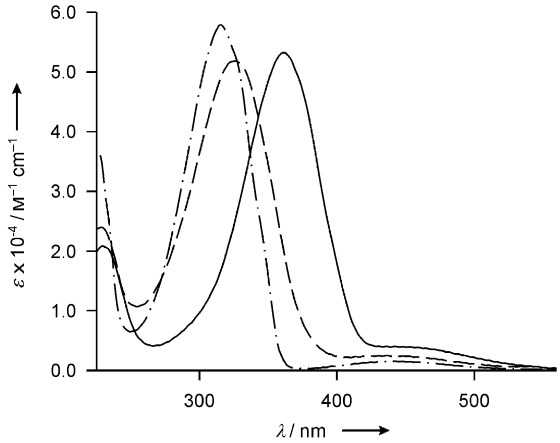

Figure 1. Absorption spectra of (*E*,*E*)-*m*-**1** (dashed line) and (*E*,*E*)-*p*-**1** (full line) in acetonitrile at room temperature. The absorption spectrum of (*E*)-azobenzene, multiplied by 2, is also shown for comparison (dashed-dotted line).

Table 1. Absorption, photochemical and electrochemical data.

	Absorption[a]		$E \rightarrow Z$ Photoreaction[a]		Electrochemistry[b,c]		
	π–π*	n–π*	π–π* irradiation		n–π* irradiation		
	λ_{max} [nm] (ε [$M^{-1}cm^{-1}$])	λ_{max} [nm] (ε [$M^{-1}cm^{-1}$])	Φ	$\%^{Z}$PSS[d,e]	Φ	$\%^{Z}$PSS[d]	E [V vs SCE][f]
(*E*)-azobenzene	316 (29000)	442 (770)	0.14	95	0.35	15	−1.38
(*E*,*E*)-*m*-**1**	326 (52000)	436 (2500)[g]	0.12	79	0.30	18	−0.86
(*E*,*E*)-*p*-**1**	361 (53000)	~450 (~4000)[g]	0.017	32	0.03	~1	−0.84; −0.85

[a] Air-equilibrated acetonitrile, 298 K. [b] Argon-purged acetonitrile with 0.05 M TEAP. [c] First reduction process of the azobenzene unit(s). [d] Fraction of (*Z*)-azo units at the photostationary state (PSS). [e] Irradiation wavelength of maximum conversion (345 nm for (*E*)-azobenzene and (*E*,*E*)-*m*-**1**, 384 nm for (*E*,*E*)-*p*-**1**). See the text for details. [f] Irreversible processes; peak potential estimated from DPV peaks. [g] Partially overlapped with the π–π* band.

Compounds (*E*,*E*)-*m*-**1** and (*E*,*E*)-*p*-**1** are not luminescent either at room temperature or in a frozen glass at 77 K, in line with the behaviour of azobenzene.[1,2]

***E*→*Z* photoisomerisation**: The $E \rightarrow Z$ photoisomerisation quantum yields and the composition of the photostationary states at selected irradiation wavelengths are reported in Table 1. The photoisomerisation of azobenzene was also studied under our experimental conditions as a control experiment. The quantum yield values determined are in agreement with those found in earlier accurate studies.[3]

Compound *(E,E)-m*-1: Figure 2 shows the absorption changes observed upon irradiation of (*E*,*E*)-*m*-**1** in its π–π* band at 365 nm. Such changes are consistent with the $E \rightarrow Z$ isomerisation of the azobenzene units of *m*-**1**. Similarly to that of (*E*)-azobenzene, the photoisomerisation of (*E*,*E*)-*m*-**1** is more efficient if irradiation is performed in the n–π* absorption band. It should be noted that since (*E*,*E*)-*m*-**1** contains *two* azobenzene units, the $E \rightarrow Z$ photoisomerisation

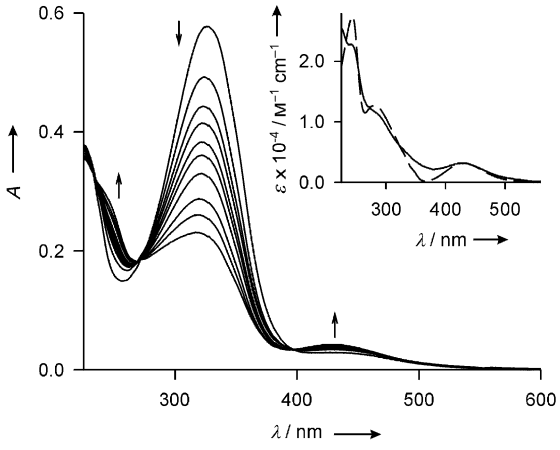

Figure 2. Absorption spectral changes on 365 nm irradiation of (*E*,*E*)-*m*-**1** (1.1×10^{-5} M in acetonitrile, room temperature). Irradiation times are 0, 0.33, 0.66, 1, 1.5, 2, 3, 5, 7.5 and 30 minutes. Inset: absorption spectrum of (*Z*,*Z*)-*m*-**1** (full line) and twice the spectrum of (*Z*)-azobenzene (dashed line).

quantum yield per azobenzene unit is actually higher than that of (*E*)-azobenzene (Table 1). Such an increased photoreactivity of the (*E*)-azo group in (*E*,*E*)-*m*-**1** can be rationalised on the basis of quantum chemical calculations (vide infra).

Since the composition of the photostationary state obtained with 365 nm light, expressed in azo units, is *E*:*Z* = 35:65, the photoreaction must span all three geometric isomers, namely, *E*,*E*, *E*,*Z* and *Z*,*Z*. The presence of a set of clean isosbestic points, which are maintained throughout the irradiation, suggests that the spectrum of (*E*,*Z*)-*m*-**1** is almost the sum of half the spectrum of (*E*,*E*)-*m*-**1** and half that of (*Z*,*Z*)-*m*-**1**, as expected for two weakly interacting chromophores. Alternative explanations for this behaviour could be based on the sequential reaction scheme $E,E \rightarrow E,Z \rightarrow Z,Z$, assuming that the quantum yield for the second photoisomerisation step is much higher than that of the first step, or considering that the absorption of one photon causes the isomerisation of both azo units. These models, however, can be discarded since they are in contrast with the behaviour observed for (*E*,*E*)-*m*-**1**, which shows a decrease of the apparent quantum yield of photoisomerisation with irradiation time, and are not in agreement with the results of the quantum chemical modelling (see below). It can therefore be concluded that, from UV-visible absorption data, only the total amount of *E* and *Z* isomeric forms of the azo units of *m*-**1** can be determined, irrespective of their belonging to the same or different molecules. As will be shown in the next section, the computed vertical excitation energies and intensities for the three isomers of *m*-**1** agree with the experimental observations. The inset of Figure 2 shows the spectrum of the final photoproduct, (*Z*,*Z*)-*m*-**1**, obtained by subtraction of the absorption spectrum of the reactant, together with the absorption spectrum of (*Z*)-azobenzene. These observations, together with the absorption behaviour and the similarities with azobenzene, indicate that *m*-**1** is composed of two weakly interacting azo units. A quantitative discussion of the electronic coupling in these bis(azo) derivatives, fully supporting the above conclusions, will be given in the next section.

For photochromic systems in which the two forms absorb in the same spectral region, such as those described here, the absorbance changes at short irradiation times must be employed for the determination of the photoreaction quantum yield. At higher photoconversions, the absorption of light by the photoproduct becomes substantial and back-photoisomerisation cannot be neglected. However, if the irradiation is performed at a wavelength at which the product exhibits a very low molar absorption coefficient relative to the reactant, the quantum yield is expected to show small changes also for higher degrees of photoconversion. An "instantaneous" apparent quantum yield for the disappearance of the *E* species can be defined [Eq (1)]:

$$\Phi_{app}(t_2) = \frac{A_\lambda^E(t_2) - A_\lambda^E(t_1)}{\varepsilon_\lambda^E - \varepsilon_\lambda^Z} V \frac{1}{N(t_2 - t_1)F^E} \quad (1)$$

in which $A_\lambda^E(t_1)$ and $A_\lambda^E(t_2)$ are the solution absorbance at irradiation time t_1 and t_2, respectively, measured at a wavelength λ at which the absorbance of the Z form is negligible, ε_λ^E and ε_λ^Z are the molar absorption coefficient of the E and Z forms, respectively, at the wavelength λ, V is the volume of irradiated solution, N is the moles of incident photons per unit time in the volume V, and F^E is the fraction of irradiation light absorbed by the E form. Figure 3 shows the changes of $\Phi_{app}(t)$, normalised to the initial quantum yield, as a function of the photoconversion, expressed as the fraction of photogenerated (Z)-azo units. It can be clearly seen that the $E \rightarrow Z$ photoisomerisation quantum yield of *m*-**1** decreases much more rapidly than that of azobenzene, especially at low conversion. For example, at a $E \rightarrow Z$ conversion of 10%, the quantum yield for (*E*,*E*)-*m*-**1** is approximately 18% lower than its initial value. Since we have checked that the $Z \rightarrow E$ photoisomerisation in (*Z*,*Z*)-*m*-**1** is not faster than that of azobenzene, such an effect cannot be ascribed to the back-photoisomerisation. Therefore, one can conclude that the photoreactivity of one azo unit in *m*-**1** depends on the isomeric form, that is, *E* or *Z*, of the neighbouring unit.[20] More specifically, the presence of a (Z)-azo unit in (*E*,*Z*)-*m*-**1** reduces the quantum yield value for the $E \rightarrow Z$ photoisomerisation of the (E)-azo unit. Note that the presence of a (Z)-azo unit in (*E*,*Z*)-*m*-**1** introduces an asymmetry in the torsional potential-energy curve that might be one of the causes of the reduced photoreactivity, since isomerisation in one of the two possible directions will be strongly hindered by steric repulsions.

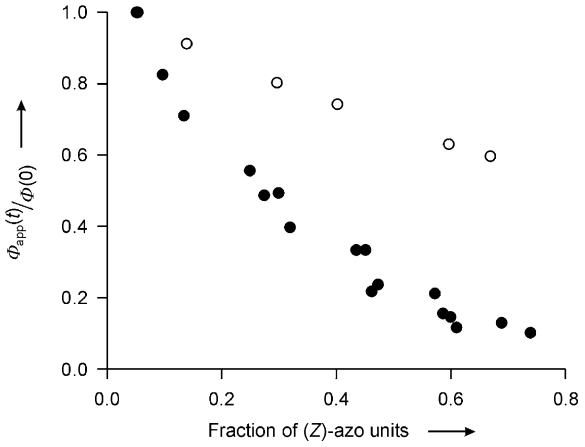

Figure 3. Changes of the instantaneous apparent quantum yield for $E \rightarrow Z$ photoisomerisation of azobenzene (empty circles) and *m*-**1** (full circles), normalised to the initial quantum yield value, as a function of the photoconversion, expressed as the fraction of photogenerated (Z)-azo units. To ensure the same spectral conditions, the measurements have been carried out on solutions with similar absorbance.

Compound (*E*,*E*)-*p*-1: The photoreactivity of (*E*,*E*)-*p*-**1** is much decreased relative to the *meta*-isomer and azobenzene; the $E \rightarrow Z$ quantum yield is only approximately 0.02 (Table 1). In irradiation experiments at 313, 334, 365 and 404 nm (Hg emission lines) very limited $E \rightarrow Z$ conversion could be achieved, the best result being about 13% on 365 nm irradiation. In the attempt to isolate the absorption spectrum of the photoproduct, an appropriate fraction of the initial absorption spectrum was subtracted to the spectrum of the photostationary state. From this calculation it can be noted that the photoproduct has an absorbance minimum at about 384 nm. Therefore, irradiation at this optimised wavelength was performed and, as expected, a higher conversion (ca. 30%) was attained. Figure 4 shows the absorption changes upon irradiation of (*E*,*E*)-*p*-**1** at 384 nm; the spectrum of the photoproduct, obtained as described above, is represented in the inset.

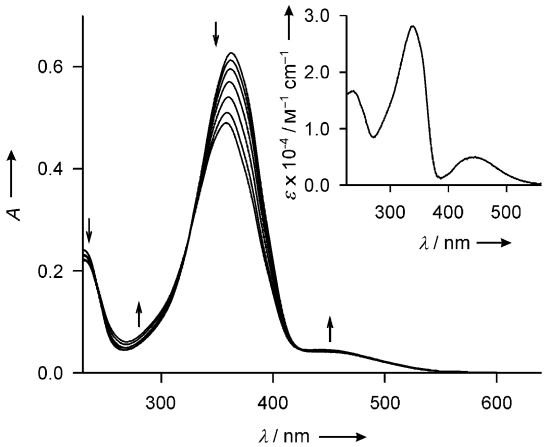

Figure 4. Absorption spectral changes on 384 nm irradiation of (*E*,*E*)-*p*-**1** (1.1×10^{-5} M in acetonitrile, room temperature). Irradiation times are 0, 2, 4, 8.5, 16, 30 and 75 minutes. Inset: absorption spectrum of the primary photoproduct.

The presence of isosbestic points may suggest behaviour similar to that of *m*-**1**, but the limited $E \rightarrow Z$ conversion does not ensure the formation of species in which both azo units have been isomerised into the Z form. Thus, it is possible that the primary photoproduct observed is mainly the *E*,*Z* isomer. This is in agreement with the spectrum shown in the inset of Figure 4, which is very different from that of (Z)-azobenzene and (*Z*,*Z*)-*m*-**1** (Figure 2, inset). In particular, the intense absorption band with maximum at approximately 340 nm may be assigned to the π–π* transition of the (E)-azo unit in the *E*,*Z* photoproduct; such a band is more similar to that found for (*E*,*E*)-*m*-**1** rather than that for (*E*,*E*)-*p*-**1**, possibly because of partial loss of electronic conjugation with the more distorted (Z)-azo unit (see the next section). This would also imply the absorption spectrum of (*E*,*Z*)-*p*-**1** is *not* the average of the spectra of (*E*,*E*)-*p*-**1** and (*Z*,*Z*)-*p*-**1**. Such a conjecture has been confirmed by consecutive irradiation experiments with light of different wavelengths and will be supported in the next section on the basis of quantum chemical calculations of excitation energies.

From the absorption spectra shown in Figure 4 it can be determined that selective irradiation of the primary photo-

product can be best carried out at 260 nm, whereby more than 50% of the incident light is absorbed by the photoproduct. Therefore, a solution of (*E*,*E*)-*p*-**1** was first irradiated at 384 nm, until the photostationary state had been reached, and subsequently irradiated at 260 nm. Upon 260 nm irradiation, the isosbestic points observed during irradiation at 384 nm are lost; new isosbestic points, slightly shifted from the previous location, appear on prolonged irradiation. The time evolution of the absorbance at 241 nm (which represents an isosbestic point for the 384 nm irradiation) during 260 nm irradiation is reported in Figure 5. A similar behaviour was observed for the other isosbestic points. Such a result can be rationalised with the following model, which involves the reactant (A), the primary photoproduct (B), and a third species (C) as the secondary photoproduct [Eq. (2)].

$$A \underset{\Phi_{-1}}{\overset{\Phi_1}{\rightleftharpoons}} B \underset{\Phi_{-2}}{\overset{\Phi_2}{\rightleftharpoons}} C \qquad (2)$$

The following zero-order kinetic equations [Eq. (3)–(5)] can be derived from the definition of the photoreaction quantum yield.

$$\frac{\Delta[A]}{\Delta t} = \Phi_{-1}(1-10^{-A_{260}})\frac{\varepsilon^{B}_{260}[B]}{A_{260}}\frac{N}{V} - \Phi_1(1-10^{-A_{260}})\frac{\varepsilon^{A}_{260}[A]}{A_{260}}\frac{N}{V} \qquad (3)$$

$$\frac{\Delta[B]}{\Delta t} = \Phi_1(1-10^{-A_{260}})\frac{\varepsilon^{A}_{260}[A]}{A_{260}}\frac{N}{V} + \Phi_{-2}(1-10^{-A_{260}})\frac{\varepsilon^{C}_{260}[C]}{A_{260}}\frac{N}{V} - (\Phi_{-1}+\Phi_2)(1-10^{-A_{260}})\frac{\varepsilon^{B}_{260}[B]}{A_{260}}\frac{N}{V} \qquad (4)$$

$$\frac{\Delta[C]}{\Delta t} = \Phi_2(1-10^{-A_{260}})\frac{\varepsilon^{B}_{260}[B]}{A_{260}}\frac{N}{V} - \Phi_{-2}(1-10^{-A_{260}})\frac{\varepsilon^{C}_{260}[C]}{A_{260}}\frac{N}{V} \qquad (5)$$

in which the symbols used have the same meaning as those in Equation (1). From a numerical solution of these equations, the photokinetic behaviour of the system can be simulated (Figure 5). The above rate equations could be used in principle to determine the unknown parameters from the fit of absorbance versus time profiles. In the present case, however, the absorbance changes are very small and there are many unknown parameters in the above equations. Thus, the simulation of Figure 5 should be regarded only as a qualitative proof that a third species, with a characteristic absorption spectrum, appears in the reaction mixture upon irradiation. On the basis of the above results, we infer that the B and C species are in fact (*E*,*Z*)-*p*-**1** and (*Z*,*Z*)-*p*-**1**.

After irradiation, *m*-**1** and *p*-**1** showed a slow (timescale of days) recovery of the original absorption bands of their *E*,*E* form if stored in the dark, indicating the occurrence of a thermal *Z*→*E* isomerisation process, similar to that of azobenzene. The influence of such a slow process on the photochemical studies presented in this work can be safely neglected.

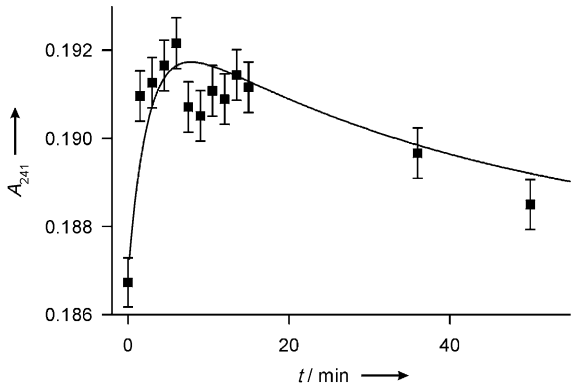

Figure 5. Time-dependent change of the absorbance at 241 nm for a solution of (*E*,*E*)-*p*-**1** (pre-irradiated at 384 nm up to a photostationary state) upon irradiation at 260 nm. The wavelength 241 nm was selected as the observation wavelength, since it is an isosbestic point for the initial 384 nm irradiation. The line shows the simulation of the absorbance change on the basis of the kinetic reaction model described in the text.

Quantum chemical modelling: To clarify the trend observed in the absorption maxima and to assist the assignment of the photoproducts, vertical excitation energies were obtained with ZINDO/1 + CIS calculations carried out at the HF/6–31G computed equilibrium geometries. The computed excitation energies of the lowest π–π* transitions are compared, in Table 2, with the correspondingly observed absorption maxima. It is seen that the agreement between observed and computed absorption maxima is very satisfactory.

To rationalise the spectroscopical and photochemical behaviour of the bis(azo) derivatives upon excitation in the π–π* region, and to quantify the degree of electronic coupling in the *m*-**1** and *p*-**1** compounds, we can analyse the electron-

Table 2. Comparison between computed and observed π–π* excitation energies.

	observed[a]	computed[b]			Wf composition
	λ_{max} [nm] (ε [$M^{-1}cm^{-1}$])	ΔE [nm] (f[c])	ΔE [eV]	Gap [eV][d]	
(*E*)-azobenzene	316 (29000)	317 (1.04)	3.92		0.70 (H→L)
(*E*,*E*)-*m*-**1**	326 (52000)	332 (1.92)	3.74	0.18	0.46 (H−1→L); 0.52 (H→L+1)
		316 (0.27)	3.92		0.62 (H→L); 0.31 (H−1→L+1)
(*E*,*E*)-*p*-**1**	361 (53000)	366 (1.89)	3.39	0.77	0.67 (H→L); 0.21(H−1→L+1)
		298 (0.00)	4.16		0.46 (H−1→L); 0.52 (H→L+1)
(*Z*)-azobenzene	282 (6300)	301 (0.27)			
(*E*,*Z*)-*m*-**1**		327 (1.18)			
		307 (0.09)			
		299 (0.17)			
(*E*,*Z*)-*p*-**1**	340 (28000)	344 (1.17)			
		300 (0.11)			
(*Z*,*Z*)-*m*-**1**	~290[e] (10000)	308 (0.31)			
		301 (0.27)			
(*Z*,*Z*)-*p*-**1**		322 (0.60)			
		297 (0.00)			

[a] Air-equilibrated acetonitrile, 298 K. [b] Vertical excitation energies ΔE from ZINDO/1 + CIS calculations. [c] Oscillator strength. [d] Energy gap between the lowest two π–π* states that would be degenerate in decoupled bis(azo) derivatives. See the discussion in the text. [e] Shoulder.

ic nature (i.e., the wavefunction compositions) of the lowest π–π* excited states. These are collected in the last column of Table 2 for the *E*,*E* isomers of the bis(azo) derivatives and for (*E*)-azobenzene.

Note that, for simplicity, in the following discussion we will focus only on the π–π* excited states with dominant π_{NN}–π* character and disregard those dominated by π_{phenyl}–π* character, which are also involved in the excited-state relaxation of azobenzene.[21] Inspection of Table 2 shows that while the lowest π–π* state of (*E*)-azobenzene is dominated by the HOMO–LUMO (H→L) excitation, owing to the presence of two azobenzene units, at least four molecular orbitals, namely the H−1, H, L and L+1 must be taken into account to describe the lowest π–π* excited states of the bis(azo) derivatives. The HF/3–21G frontier molecular orbitals are given in Figure 6 for (*E*)-azobenzene and in Figures 7 and 8 for (*E*,*E*)-*m*-**1** and (*E*,*E*)-*p*-**1**, respectively. Note

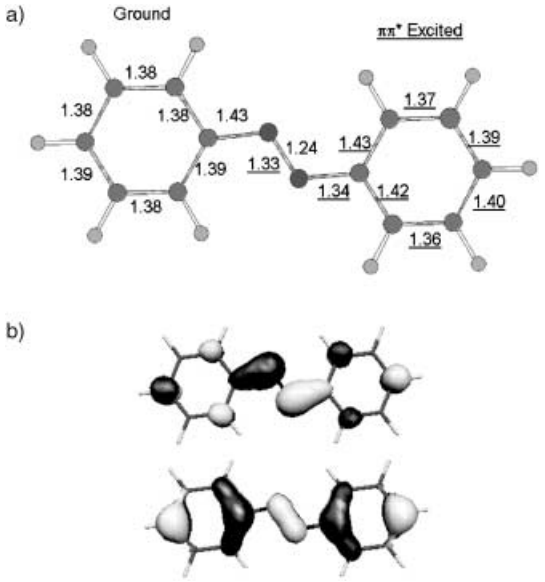

Figure 6. (*E*)-azobenzene: a) Ground state (HF/3-21G) and lowest π–π* excited state (CIS/3-21G, underlined) equilibrium structures (bond lengths in Å). b) Frontier orbitals computed at the ground state geometry.

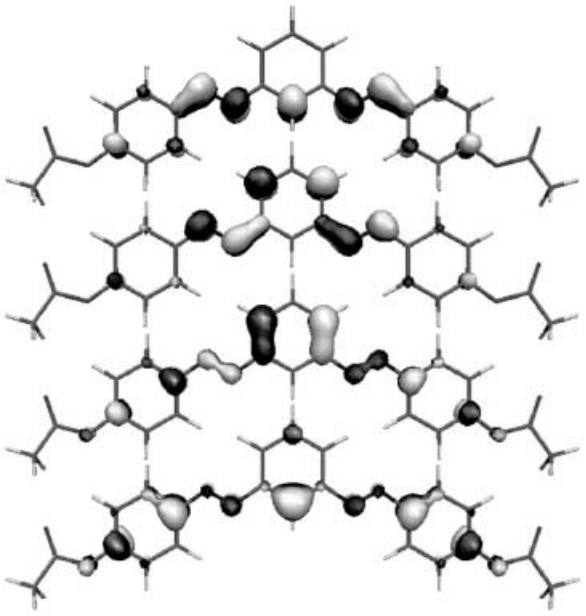

Figure 7. HF/3-21G frontier orbitals of (*E*,*E*)-*m*-**1** computed at the equilibrium structure of the ground state. From bottom to top: H−1, H, L, L+1 molecular orbitals.

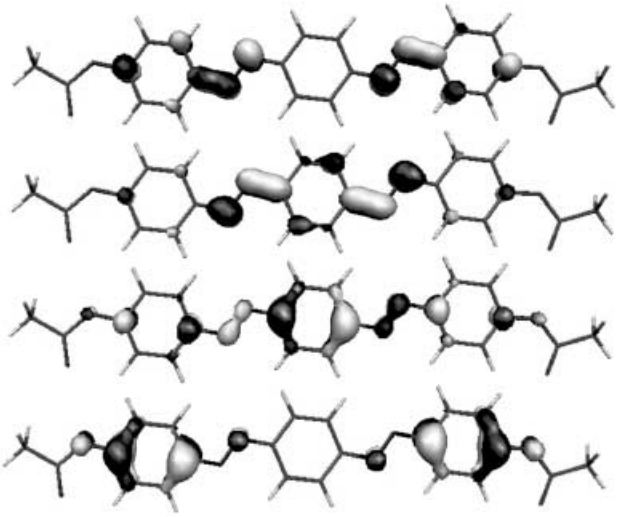

Figure 8. HF/3-21G frontier orbitals of (*E*,*E*)-*p*-**1** computed at the equilibrium structure of the ground state. From bottom to top: H−1, H, L, L+1 molecular orbitals.

that ZINDO/1 and HF/3–21G methods predict exactly the same order and shape for the π_{NN} molecular orbitals. The frontier orbitals of both bis(azo) derivatives are delocalised, as are the excited states built from them. Similar delocalisation does not imply, however, similar conjugation efficiency, since the latter is determined by the magnitude of the electron–electron coupling and is manifested by the energy splitting of the molecular orbitals. The increased degree of coupling, or conjugation, in (*E*,*E*)-*p*-**1** versus (*E*,*E*)-*m*-**1** can be clearly seen from Scheme 1 in which the energies of the HF/3–21G frontier orbitals are reported for (*E*)-azobenzene and the two bis(azo) derivatives. The H, H−1 and L, L+1 molecular orbitals, (and similarly the lowest two π–π* states) would be degenerate for two fully decoupled azobenzene units, while they are energetically separated in the conjugated compounds studied here and the splitting is larger for the *para* compound.

The four-configuration nature of the lowest two π–π* of the bis(azo) derivatives implies that a discussion of their photophysical and photochemical properties cannot be based simply on the inspection of the HOMO and LUMO orbitals. For instance, in contrast with (*E*)-azobenzene and (*E*,*E*)-*p*-**1**, the lowest π–π* excited state of (*E*,*E*)-*m*-**1** is dominated by the (H−1→L) and (H→L+1) excitations. The larger energy separation computed for the lowest two π–π* excited states of (*E*,*E*)-*p*-**1** (0.77 eV, see Table 2) with respect to (*E*,*E*)-*m*-**1** (0.18 eV) is also a consequence of the more efficient conjugation in the former. We can now inter-

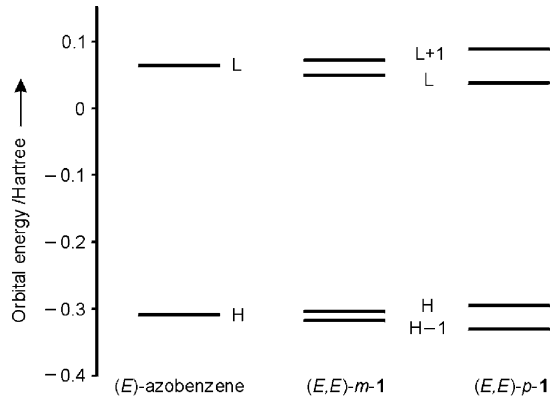

Scheme 1. Energies of the HF/3-21G frontier orbitals of (*E*)-azobenzene, (*E*,*E*)-*m*-**1** and (*E*,*E*)-*p*-**1** bis(azo) derivatives.

pret the different spectroscopic behaviour of (*E*,*E*)-*p*-**1** with respect to (*E*,*E*)-*m*-**1** in terms of the stronger coupling, in the former, between the lowest two π–π* states that would be degenerate for a decoupled bis(azo) derivative. Because of such coupling, the lowest of the two π–π* excited states is pushed at much lower energies relative to the corresponding state in (*E*,*E*)-*m*-**1**. Conversely, the second lowest π–π* state is found at much higher energies in (*E*,*E*)-*p*-**1** (4.16 eV) with respect to (*E*,*E*)-*m*-**1** (3.92 eV, see Table 2). As a result, the absorption spectrum of (*E*,*E*)-*m*-**1** almost overlaps with twice the spectrum of a single (*E*)-azobenzene unit. The spectroscopic features of the *E*,*Z* and *Z*,*Z* isomers can be interpreted with similar considerations.

As will be shown below, the larger energy separation between the lowest two π–π* excited states in (*E*,*E*)-*p*-**1** is also associated with its reduced photoisomerisation efficiency.

To understand the remarkably different photoisomerisation efficiency of the two (*E*,*E*)-bis(azo) derivatives, we carried out ab initio calculations (CIS/3–21G) of geometry optimisation and obtained the relaxed structure of the lowest π–π* state. The computed equilibrium structure of the π–π* state and, for comparison, of the ground state of (*E*)-azobenzene are shown in Figure 6. It is seen that the N–N bond length increases from 1.24 Å in the ground state to 1.33 Å in the excited state. The lengthening of this bond is associated with the efficient photoisomerisation reaction. In Figure 9 the computed equilibrium structures of the ground and lowest π–π* excited state of the two (*E*,*E*)-bis(azo) derivatives are shown. The π–π* state of (*E*,*E*)-*p*-**1** relaxes to a delocalised structure characterised by two equal N–N bond lengths of 1.30 Å. The N–N elongation upon excitation (1.24 Å in the ground state) is considerably reduced with respect to (*E*)-azobenzene and this accounts for its reduced photoisomerisation efficiency. Indeed, the increased barrier to isomerisation will favour other deactivation channels involving, for instance, phenyl-ring dynamics. The wavefunction nature of this excited state does not change along the relaxation path, and the frontier orbitals of (*E*,*E*)-*p*-**1** computed at the equilibrium geometry of the π–π* state are virtually identical to those depicted in Figure 8. In contrast, the π–π* state of (*E*,*E*)-*m*-**1** changes nature along the relaxation path, as shown by the wavefunction composition and molecular orbital shapes (see Figure 10), and relaxes to a localised

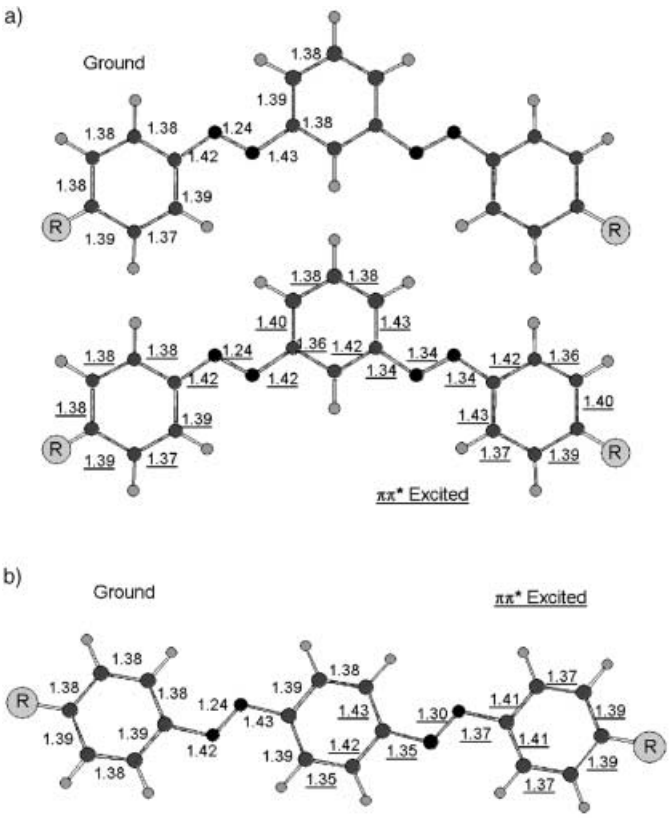

Figure 9. Computed equilibrium structures of the ground state (HF/3-21G) and lowest π–π* excited state (CIS/3-21G, underlined) for a) (*E*,*E*)-*m*-**1** and b) (*E*,*E*)-*p*-**1**. Bond lengths are in Å.

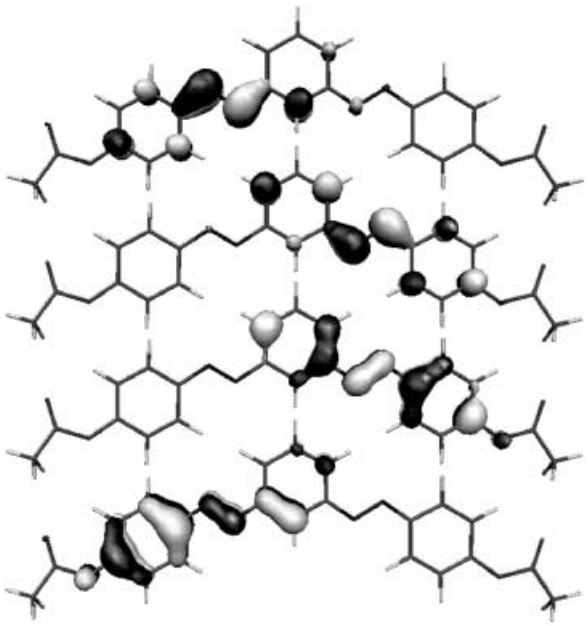

Figure 10. HF/3-21G frontier orbitals of (*E*,*E*)-*m*-**1** computed at the equilibrium structure of the lowest π–π* excited state. From bottom to top: H−1, H, L, L+1 molecular orbitals.

structure characterised by two N–N bond lengths remarkably different. Upon relaxation the molecule loses the σ_v symmetry plane. As a result, one N–N remains virtually un-

changed and the other increases to 1.34 Å. The remarkable elongation of a single N–N bond, which becomes even longer than that of excited azobenzene (1.33 Å) supports, on the one hand, the increased photoisomerisation efficiency of (*E*,*E*)-*m*-**1** relative to (*E*)-azobenzene and, on the other, it suggests a sequential *E*,*E*→*E*,*Z*→*Z*,*Z* photoisomerisation mechanism. The different excited state relaxation of (*E*,*E*)-*m*-**1** with respect to (*E*,*E*)-*p*-**1** can be ascribed to the presence of a strong electron–phonon coupling mediated by the asymmetric NN stretching vibrational mode as shown in Scheme 2. This vibrational mode drives the localisation of

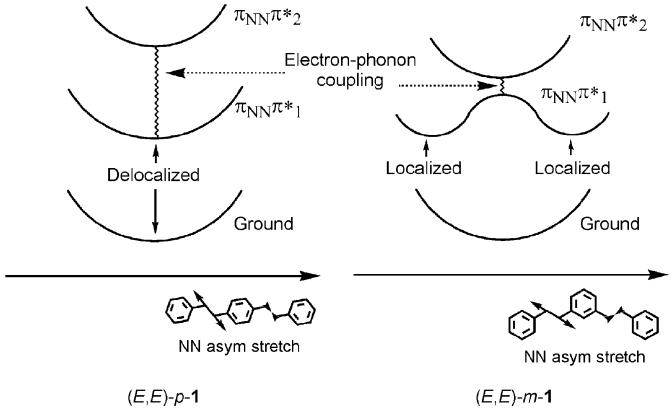

Scheme 2. Schematic representation of the delocalised [(*E*,*E*)-*p*-**1**] and localised [(*E*,*E*)-*m*-**1**] relaxed structure of the lowest π–π* state of the bis(azo) derivatives. The approximate shape of the vibrational mode coupling the two π–π* states is also shown.

the excitation in the lowest π–π* state by coupling and mixing the almost degenerate couple of π_{NN}–π* states. Such mechanism is not effective in (*E*,*E*)-*p*-**1** owing to the large energy difference between the two π_{NN}–π* states. In summary, it is the balance between the electron–electron interaction (conjugation) and the electron–vibration interaction that drives the localised or delocalised character of the π–π* excited state, which, in turn, affects the photoisomerisation efficiency of the (*E*,*E*)-bis(azo) derivatives.

Electrochemical behaviour: The electrochemical properties of (*E*)-azobenzene have been the subject of a detailed investigation.[22] In our conditions, azobenzene shows two not fully reversible reduction processes, and two irreversible oxidation processes. Compounds (*E*,*E*)-*m*-**1** and (*E*,*E*)-*p*-**1** exhibit poorly reversible reduction processes and irreversible oxidation processes, suggesting a very complex electrochemical behaviour.[23] The peaks appearing at fairly negative potentials (below −1.6 V), not observed for azobenzene, are most likely related to the reduction of the ester side groups.[24] For the sake of simplicity, we will discuss only the first reduction process (Table 1), which is assigned to the uptake of one electron per each azobenzene unit.

Figure 11 shows the CV peaks corresponding to the first reduction process of (*E*,*E*)-*m*-**1** and (*E*,*E*)-*p*-**1** in acetonitrile. The first reduction for both the bis(azo) compounds occurs at a less negative potential relative to azobenzene, owing to the presence of 1) an extended π system, which lowers the

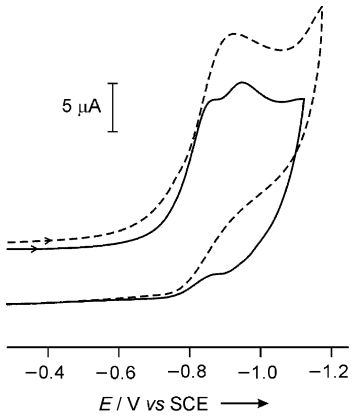

Figure 11. Cyclic voltammetric curves for the first reduction process of the azobenzene units of (*E*,*E*)-*m*-**1** (dashed line) and (*E*,*E*)-*p*-**1** (full line). Conditions: 4×10^{-4} M Ar-purged acetonitrile, room temperature, 0.05 M TBAP; scan rate = 200 mV s.

energy of the LUMO (see Scheme 1 and the discussion in the previous section), and 2) electron-withdrawing ester substituents. It is interesting to note that the first peak of the *para* derivative is split into two processes, while the *meta* compound shows a single peak. Apparently, uptake of one electron by (*E*,*E*)-*p*-**1** affects the reduction potential of the resulting anion, while this does not happen for (*E*,*E*)-*m*-**1**. A simple, qualitative explanation for the different electrochemical behaviour can be inferred by inspecting the LUMO orbital splitting in Scheme 1. Indeed, the small energy separation between the LUMO and LUMO+1 orbitals computed for (*E*,*E*)-*m*-**1** implies similar reduction potentials for both reduction processes, whilst the considerably larger splitting computed for (*E*,*E*)-*p*-**1** supports the splitting measured for the *para* compound. Furthermore, if we assume that the anion formed by the first reduction process behaves in a similar fashion to the lowest π–π* state of the neutral molecule, we can provide an additional justification for the observed electrochemical behaviour. Only one peak is observed for (*E*,*E*)-*m*-**1**, due to the localised nature of the reduced state; this leaves the second azobenzene unit and its reduction potential almost unchanged with respect to the neutral molecule. In contrast, two peaks are observed for (*E*,*E*)-*p*-**1**, due to the delocalised nature of the anion, which is a new species characterised by its own reduction potential. Thus, once more, the experimental and computational results reinforce each other and indicate a more efficient conjugation between the azo units in the *para* than in the *meta* compound.

Conclusion

The UV-visible absorption spectra, the *E*→*Z* photoisomerisation reaction and the electrochemical properties of two bis(azo) derivatives, (*E*,*E*)-*m*-**1** and (*E*,*E*)-*p*-**1**, have been investigated. These two compounds are composed of a pair of azobenzene units sharing one of their phenyl rings, and differ only for the relative position of the two azo groups on the central phenyl ring. In summary, the absorption spectra

and photoisomerisation properties of (*E*,*E*)-*m*-**1** are similar to those of (*E*)-azobenzene, while (*E*,*E*)-*p*-**1** exhibits a substantial red shift in the absorption bands and a much decreased photoreactivity. From a detailed study on the quantum yield for the $E \rightarrow Z$ photoisomerisation reaction in (*E*,*E*)-*m*-**1**, it can be observed that the photoreactivity of an (*E*)-azo unit in an *m*-**1** molecule is quenched by a neighbouring (*Z*)-azo unit. The three geometric isomers of *m*-**1**, namely *E*,*E*, *E*,*Z* and *Z*,*Z*, cannot be resolved by absorption spectroscopy, whereas a careful analysis of the absorption changes observed upon photoisomerisation of *p*-**1** reveals the presence of three distinct species. These observations can be rationalised in terms of a stronger electronic communication of the two azo units in *p*-**1** with respect to *m*-**1**.

Quantum chemical calculations of molecular orbitals at the ground-state geometry show similar delocalisation for *p*-**1** and *m*-**1**, but the computed energies do indeed confirm a larger electronic coupling for the *para* compound. Accordingly, the computed vertical excitation energies closely follow the observed behaviour. The balance between the electron–electron coupling (dominant in the *para* compound) and the electron–vibration coupling (dominant in the *meta* compound) determines the delocalised (*p*-**1**) or localised (*m*-**1**) nature of the relaxed π–π* excited state computed for the *E*,*E* isomers and accounts for the reduced photoisomerisation efficiency of *p*-**1**.

Similar considerations on the reduced forms of *p*-**1** and *m*-**1** explain the results of electrochemical experiments. Therefore, *m*-**1** can be considered closer to a two-component species composed of weakly interacting azobenzene units, whereas *p*-**1** is better described as a large molecule[25] in which the two chromophoric groups are electronically coupled.

These results may be useful for the design of novel oligomers and polymers, based on the azobenzene unit, with predetermined photoreactivity.

Experimental Section

General methods: Reagents and dry solvents were purchased from Fluka unless otherwise noted. (*E*)-Azobenzene was purchased from Aldrich. NMR spectra were recorded with a Varian Gemini 200 instrument. ESI-MS spectra were obtained with a Micromass ZMD 4000 spectrometer.

The absorption and luminescence spectra were recorded with a Perkin–Elmer λ40 spectrophotometer and an LS 50 spectrofluorimeter, respectively, in air-equilibrated acetonitrile (Merck Uvasol®) at room temperature, with concentrations ranging from 1×10^{-6} to 1×10^{-5} M, contained in 1 cm quartz cells. Experimental errors: wavelengths, ±1 nm; molar absorption coefficients, 5%.

Photochemical reactions were performed on the same solutions, thoroughly stirred, by using either a Hanau Q400 medium pressure Hg lamp (150 W) or the Xe lamp (150 W) of a Perkin–Elmer 650–10S spectrofluorimeter. In the first case, selection of the desired irradiation wavelength (313, 334, 365, 405 or 436 nm) was accomplished by the use of appropriate combinations of interference, broad-band and cut-off filters, while in the second case the monochromator of the instrument (band-pass = 5 nm) was employed. The number of incident photons, determined by ferrioxalate actinometry[26] in its micro version,[27] was between 10^{-8} and 10^{-6} $Nh\nu$ min^{-1}. The $E \rightarrow Z$ quantum yields for π–π* (λ_{irr} = 313 or 365 nm) and *n*–π* (λ_{irr} = 436 nm) irradiation were determined from the disappearance of the π–π* absorption band of the reactant at low conversion percentages (< 10%; if necessary, extrapolation to $t = 0$ was made). The fraction of light transmitted at the irradiation wavelength was taken into account in the calculation of the yields. Where possible, the composition of the photostationary state and the absorption spectrum of the photoproduct were evaluated by a calibrated subtraction of a fraction of the initial absorption spectrum from the absorption spectrum at the photostationary state. The $Z \rightarrow E$ photoisomerisation experiments on (*Z*,*Z*)-*m*-**1** were carried out with samples obtained by exhaustive irradiation of (*E*,*E*)-*m*-**1** and contained at least 60% of the *Z*,*Z* isomer. The experimental error on the quantum yield values was estimated to be 10% for π–π* irradiation, and 20% for *n*--π* irradiation.

Electrochemical experiments were carried out by employing cyclic voltammetry (CV) and differential pulse voltammetry (DPV) techniques in argon-purged acetonitrile (Romil HiDry®) at room temperature, with an Autolab 30 multipurpose instrument interfaced to a PC. The working electrode was a glassy carbon electrode (Amel; 0.07 cm^2); its surface was routinely polished with a 0.3 μm alumina/water slurry on a felt surface, immediately prior to use. The counterelectrode was a Pt wire, separated from the solution by a frit; an Ag wire was employed as a quasi-reference electrode, and ferrocene was present as an internal standard. The concentration of the compounds examined was 4×10^{-4} M; tetrabutylammonium hexafluorophosphate (TBAP) 0.05 M was added as supporting electrolyte. Cyclic voltammograms were obtained at sweep rates varying from 20 to 500 mV s^{-1}; differential pulse voltammograms were recorded at sweep rates of 20 and 4 mV s^{-1} with a pulse height of 75 or 10 mV, respectively, and a duration of 40 ms. The potential window examined was from −2 to +2 V versus SCE. The experimental error on the potential values was estimated to be 10 mV.

Synthesis of (*E*,*E*)-*p*-1: 4′-Aminoacetanilide (5.41 g, 36 mmol) was dissolved in water (13 mL) and 37% HCl (13 mL). The mixture was cooled to 0 °C and diazotised by adding a cold solution of $NaNO_2$ (2.61 g, 37.8 mmol) in water (7 mL) at such a rate as to keep the temperature of the reaction mixture below 2 °C. A few crystals of urea were then added and the mixture was slowly transferred into a cooled solution of phenol (3.29 g, 35 mmol) and NaOH (7.0 g, 0.17 mol) in water (25 mL). The slurry was allowed to warm to room temperature and carefully acidified with conc. HCl to about pH 6. Filtration of the resulting mixture afforded 4-(4′-hydroxyphenylazo)acetanilide as an orange-brown solid in a 76% yield. ESI-MS (MeOH): *m*/*z*: 256 $[M+H]^+$; ^{1}H NMR (200 MHz, [D$_6$]DMSO): δ = 2.11 (s, 3H), 6.94 (m, 2H), 7.78 (m, 6H), 10.23 (s, 1H), 10.25 ppm (s, 1H).

4-(4′-Hydroxyphenylazo)acetanilide (6.97 g, 27.3 mmol) was dissolved in 10% NaOH (350 mL) refluxed for 2 h. The mixture was then cooled to room temperature and the pH was adjusted to 6 with conc. HCl. The resulting precipitate was filtered, washed with water and dried in vacuo to afford 4-(4′-hydroxyphenylazo)aniline as pale brown solid (86%). The compound was sufficiently pure to be used in the subsequent step without any further purification. ESI-MS (MeOH): *m*/*z*: 214 $[M+H]^+$; ^{1}H NMR (200 MHz, $CDCl_3$): δ = 4.0 (br s, 2H), 5.07 (s, 1H), 6.68 (m, 2H), 6.91 (m, 2H), 7.79 ppm (m, 4H).

4-(4′-Hydroxyphenylazo)aniline (4.95 g, 23.2 mmol) was suspended in water (15 mL) and conc. HCl (8.4 mL); the mixture was then cooled to 0 °C. A cold solution of $NaNO_2$ (1.61 g, 23.3 mmol) in water (4 mL) was added at such a rate to keep the temperature below 3 °C. The addition was stopped when iodine-starch paper gave a positive test. A few crystals of urea added and the mixture was slowly transferred into a cooled (0 °C) solution of phenol (2.18 g, 23.2 mmol) and NaOH (4.65 g, 116 mmol) in water (18 mL). When the addition was complete, the resulting viscous dark brown suspension was allowed to reach room temperature. The mixture was made slightly acidic with conc. HCl and filtered. The precipitate was washed with water and dried in vacuo. The filtrate was extracted with diethyl ether and the organic layer was dried over Na_2SO_4, concentrated in vacuo and added to the precipitate. The solid was purified by column chromatography over silica gel (petroleum ether/ethyl acetate 7:3 as the eluent) and the product with R_f = 0.2 was collected. 1,4-bis(4′-hydroxyphenylazo)benzene was thus obtained as an orange solid in a 76% yield. ESI-MS (MeOH): *m*/*z*: 317 $[M-H]^-$; ^{1}H NMR (200 MHz, [D$_6$]DMSO): δ = 6.96 (m, 4H), 7.85 (m, 4H), 7.98 (s, 4H), 10.42 ppm (s, 2H); ^{13}C NMR (200 MHz, [D$_6$]DMSO): δ = 115.96 (CH), 123.13 (CH), 125.04 (CH), 145.32 (C), 152.62 (C), 161.22 ppm (C).

(−)-Camphanic acid chloride (300 mg, 1.3 mmol) was quickly added to a solution of 1,4-bis(4′-hydroxyphenylazo)benzene (110 mg, 0.35 mmol) and redistilled Et_3N (0.15 mL) in dry CH_3CN (5 mL) under inert atmosphere. The mixture was allowed to react for 2 h at room temperature and reduced to dryness in vacuo. The residue was redissolved in $CHCl_3$ (30 mL) and washed with 5% $NaHCO_3$ (3×30 mL) and water (15 mL). The resulting organic phase was dried over Na_2SO_4, the solvent was removed by distillation and the crude was purified by chromatography on silica gel (eluent: petroleum ether/ethyl acetate 6:4). Compound (*E*,*E*)-*p*-**1** was obtained as an orange solid in a 45% yield. ^{1}H NMR (200 MHz, $CDCl_3$): δ = 1.13 (s,6H), 1.17 (s,6H), 1.18 (s, 6H), 1.70–1.87 (m, 2H), 1.94–2.10 (m, 2H), 2.16–2.30 (m, 2H), 2.51–2.68 (m, 2H), 7.31 (m, 4H), 7.99–8.09 ppm (m, 8H); elemental analysis calcd (%) for $C_{38}H_{38}N_4O_8$ (678.74): C 67.24, H 5.64, N 8.25; found: C 67.10, H 5.59, N 8.18.

Synthesis of (*E*,*E*)-*m*-1: The preparation is analogous to that described for (*E*,*E*)-*p*-**1**. Spectral data for the corresponding derivatives are reported:

3-(4′-Hydroxyphenylazo)acetanilide: ESI-MS (MeOH): *m*/*z*: 256 $[M+H]^+$.

3-(4′-Hydroxyphenylazo)aniline: ESI-MS (MeOH): *m*/*z*: 214 $[M+H]^+$.

1,3-Bis(4′-hydroxyphenylazo)benzene: ESI-MS (MeOH): *m*/*z*: 317 $[M-H]^-$; ^{1}H NMR (200 MHz, $CDCl_3$): δ = 6.97 (m, 4H), 7.63 (t, *J* = 8.0 Hz, 1H), 7.9–8 (m, 6H), 8.36 ppm (t, *J* = 1.9 Hz, 1H).

*(E,E)-m-**1***: ^{1}H NMR (200 MHz, $CDCl_3$): δ = 1.15 (s,6H), 1.18 (s,6H), 1.19 (s, 6H), 1.71–1.87 (m, 2H), 1.94–2.10 (m, 2H), 2.17–2.32 (m, 2H), 2.52–2.68 (m, 2H), 7.33 (m, 4H), 7.69 (t, 1H), 8.00–8.09 (m, 6H), 8.44 ppm (t, 1H); elemental analysis calcd (%) for $C_{38}H_{38}N_4O_8$ (678.74): C 67.24, H 5.64, N 8.25; found: C 67.11, H 5.60, N 8.20.

Computational methods: Ground-state equilibrium structures of the three geometric isomers (*E*,*E*, *E*,*Z* and *Z*,*Z*) of *meta*- and *para*-bis(azo) derivatives and of the two isomers (*E* and *Z*) of azobenzene were optimised at HF/6–31G and HF/3–21G levels of theory. For simplicity, camphanic ester side groups were replaced by acetate groups in the calculations. The HF/6–31G equilibrium geometries were employed to calculate electronic excitation energies with the ZINDO/1 semi-empirical hamiltonian[28] combined with configuration interaction singles (CIS) calculations, which included the highest 20 occupied and lowest 20 unoccupied (20×20) molecular orbitals (MOs). In order to obtain a qualitative picture of the π–π* excited-state geometry relaxation, excited-state geometry optimisations were performed at CIS/3–21G level of theory. CIS calculations with moderate basis sets are known to overestimate excitation energies, but provide a reliable description of the geometry relaxation for excited states dominated by single excitations. Given the large dimension of the molecules investigated, the orbital space was restricted to 10×10 for (*E*,*E*) -*m*-**1** and *p*-**1** and to 6×6 for (*E*)-azobenzene. All the calculations were carried out with the Gaussian 98 suite of programs.[29] The visual program Molekel[30] was employed to produce molecular orbitals pictures.

Acknowledgments

This research was supported by MIUR (PRIN programs), FIRB (Nomade project) and the University of Bologna (Funds for Selected Research Topics). F.C. contributed to this work as research student from the École Normale Supérieure, Paris, which he gratefully acknowledges. We are indebted with Giorgio Orlandi and Sandra Monti for useful discussions.

[1] H. Rau in *Photochromism: Molecules and Systems* (Eds.: H. Dürr, H. Bouas-Laurent), Elsevier, Amsterdam, **2003**, Chapter 4.
[2] J. Griffiths, *Chem. Soc. Rev.* **1972**, *1*, 481.
[3] P. Bortolus, S. Monti, *J. Phys. Chem.* **1979**, *83*, 648, and references therein.
[4] The mechanism of *E*→*Z* photoisomerisation of azobenzene was extensively investigated in the past (ref. [1]) and has recently received a renewed attention. See ref. [21] and: a) T. Fujino, T. Tahara, *J. Phys. Chem. A* **2000**, *104*, 4203; b) T. Fujino, S. Y. Arzhantsev, T. Tahara, *J. Phys. Chem. A* **2001**, *105*, 8123; c) T. Fujino, S. Y. Arzhantsev, T. Tahara, *Bull. Chem. Soc. Jpn.* **2002**, *75*, 1031; d) L. Gagliardi, G. Orlandi, F. Bernardi, A. Cembran, M. Garavelli, *Theor. Chem. Acc.*, in press.
[5] a) A. Natansohn, P. Rochon, *Chem. Rev.* **2002**, *102*, 4139; b) G. Sudesh Kumar, D. C. Neckers, *Chem. Rev.* **1989**, *89*, 1915.
[6] For a recent interesting example, see: Y. Lu, M. Nakano, T. Ikeda, *Nature* **2003**, *425*, 145.
[7] T. Ikeda, A. Kanazawa in *Molecular Switches* (Ed.: B. L. Feringa), Wiley-VCH, Weinheim, **2001**, Chapter 12.
[8] a) O. Pieroni, A. Fissi, N. Angelini, F. Lenci, *Acc. Chem. Res.* **2001**, *34*, 9; b) I. Willner, B. Willner in *Molecular Switches* (Ed.: B. L. Feringa), Wiley-VCH, Weinheim, **2001**, Chapter 6; c) F. Ciardelli, O. Pieroni in *Molecular Switches* (Ed.: B. L. Feringa), Wiley-VCH, Weinheim, **2001**, Chapter 13.
[9] For representative examples, see: a) A. Archut, F. Vögtle, L. De Cola, G. C. Azzellini, V. Balzani, P. S. Ramanujam, R. H. Berg, *Chem. Eur. J.* **1998**, *4*, 699; b) D. M. Junge, D. V. McGrath, *J. Am. Chem. Soc.* **1999**, *121*, 4912; c) R. M. Sebastian, J. C. Blais, A. M. Caminade, J.-P. Majoral, *Chem. Eur. J.* **2002**, *8*, 2172.
[10] a) V. Balzani, F. Scandola, *Supramolecular Photochemistry*, Horwood, Chichester, **1991**, Chapter 7; b) S. Shinkai in *Molecular Switches* (Ed.: B. L. Feringa), Wiley-VCH, Weinheim, **2001**, Chapter 9.
[11] For early, representative examples, see: a) A. Ueno, H. Yoshimura, R. Saka, T. Osa, *J. Am. Chem. Soc.* **1979**, *101*, 2779; b) S. Shinkai, T. Nakaji, Y. Nishida, T. Ogawa, O. Manabe, *J. Am. Chem. Soc.* **1980**, *102*, 5860.
[12] S. Kawata, Y. Kawata, *Chem. Rev.* **2000**, *100*, 1777.
[13] V. Balzani, A. Credi, M. Venturi, *Molecular Devices and Machines—A Journey Into the Nano World*, Wiley-VCH, Weinheim, **2003**.
[14] For a recent example of a single-molecule optomechanical device based on azobenzene, see: T. Hugel, N. B. Holland, A. Cattani, L. Moroder, M. Seitz, H. E. Gaub, *Science* **2002**, *296*, 1103.
[15] Representative examples: a) S. Shinkai, O. Manabe, *Top. Curr. Chem.* **1984**, *121*, 67; b) G. Ritter, G. Häfelinger, E. Lüddecke, H. Rau, *J. Am. Chem. Soc.* **1989**, *111*, 4627; c) N. Tamaoki, K. Koseki, T. Yamaoka, *Angew. Chem.* **1990**, *102*, 66; *Angew. Chem. Int. Ed. Engl.* **1990**, *29*, 105; d) F. Vögtle, W. M. Müller, U. Müller, M. Bauer, K. Rissanen, *Angew. Chem.* **1993**, *105*, 1356; *Angew. Chem. Int. Ed. Engl.* **1993**, *32*, 1295; e) O. Röttger, H. Rau, *Mol. Cryst. Liq. Cryst. Sci. Technol. Sect. A* **1994**, *246*, 143; f) A. Bencini, M. A. Bernardo, A. Bianchi, M. Ciampolini, V. Fusi, N. Nardi, A. J. Parola, F. Pina, B. Valtancoli, *J. Chem. Soc. Perkin Trans. 2* **1998**, 413.
[16] Compounds related to those object of this study, with appropriate substituent groups, owing to their photochemical stability, are widely employed as dyes. Commercial names are, for example, Bismarck Brown R and Sudan 403. To the best of our knowledge, no information is available on photoreactive conjugated bis(azo) compounds.
[17] Unfortunately, the pitches of the cholesteric phases obtained by doping the compounds (*E*,*E*)-*p*-**1** and (*E*,*E*)-*m*-**1** in several nematic phases do not change to an appreciable extent during the photoisomerisation process. Furthermore, the circular dichroism spectroscopy in ordinary solutions does not give any evidence of formation of skewed, helicoidal conformations of the solute molecules [O. Pandoli, Laurea Thesis, University of Bologna (Italy), **2003**]. For a recent successful bis(azo) chiral photochemical switch for liquid crystal doping, see: S. Pieraccini, S. Masiero, G. P. Spada, G. Gottarelli, *Chem. Commun.* **2003**, 598.
[18] a) C. Ruslim, K. Ichimura, *J. Mater. Chem.* **1999**, *9*, 673; b) C. Ruslim, K. Ichimura, *J. Mater. Chem.* **2000**, *10*, 2704.
[19] For an early report on the absorption spectra of related compounds, see: K. Ueno, *J. Am. Chem. Soc.* **1952**, *74*, 4508.
[20] A similar effect has recently been observed in a symmetric biphotochromic system consisting of two naphthopyran units. See: W. Zhao, E. M. Carreira, *J. Am. Chem. Soc.* **2002**, *124*, 1582.
[21] T. Schultz, J. Quenneville, B. Levine, A. Toniolo, T. J. Martinez, S. Lochbrunner, M. Schmitt, J. P. Shaffer, M. Z. Zgierski, A. Stolow, *J. Am. Chem. Soc.* **2003**, *125*, 8098.
[22] J. L. Sadler, A. J. Bard, *J. Am. Chem. Soc.* **1968**, *90*, 1979.

[23] A. M. Shams-El Din, T. M. H. Saber, N. M. Abed, *J. Electroanal. Chem.* **1969**, *21*, 377.
[24] *Organic Electrochemistry* (Eds.: H. Lund, O. Hammerich), Dekker, New York, **2001**.
[25] a) V. Balzani, F. Scandola, *Supramolecular Photochemistry*, Horwood, Chichester, **1991**, Chapter 3; b) V. Balzani, A. Credi, M. Venturi, *Chem. Eur. J.* **2002**, *8*, 5524.
[26] C. G. Hatchard, C. A. Parker, *Proc. R. Soc. London Ser. A* **1956**, *253*, 518.
[27] E. Fischer, *EPA Newsl.* **1984**, *20*, 33.
[28] A. D. Bacon, M. C. Zerner, *Theo. Chim. Acta* **1979**, *53*, 21.
[29] Gaussian 98 (revision A.7), M. J. Frisch, G. W. Trucks, H. B. Schlegel, G. E. Scuseria, M. A. Robb, J. R. Cheeseman, V. G. Zakrzewski, J. A. Montgomery, Jr., R. E. Stratmann, J. C. Burant, S. Dapprich, J. M. Millam, A. D. Daniels, K. N. Kudin, M. C. Strain, O. Farkas, J. Tomasi, V. Barone, M. Cossi, R. Cammi, B. Mennucci, C. Pomelli, C. Adamo, S. Clifford, J. Ochterski, G. A.Petersson, P. Y. Ayala, Q. Cui, K. Morokuma, D. K. Malick, A. D. Rabuck, K. Raghavachari, J. B. Foresman, J. Cioslowski, J. V. Ortiz, A. G. Baboul, B. B. Stefanov, G. Liu, A. Liashenko, P. Piskorz, I. Komaromi, R. Gomperts, R. L. Martin, D. J. Fox, T. Keith, M. A. Al-Laham, C. Y. Peng, A. Nanayakkara, C. Gonzalez, M. Challacombe, P. M. W. Gill, B. Johnson, W. Chen, M. W. Wong, J. L. Andres, C. Gonzalez, M. Head-Gordon, E. S. Replogle, J. A. Pople, Gaussian, Inc., Pittsburgh PA, **1998**.
[30] Molekel Version 4.3, http://www.cscs.ch/molekel/; S. Portmann, H. P. Lüthi, *Chimia* **2000**, *54*, 766.

Received: October 1, 2003
Revised: December 8, 2003 [F5590]

